Nuclear Physics B261 (1985) 239–248


# ESTIMATION OF THE FADDEEV-POPOV SPECTRAL DENSITY AND DETERMINANT

J.L. BALDUZ, R.E. CUTKOSKY and W. TSAO*

*Physics Department, Carnegie-Mellon University, Pittsburgh, PA 15213, USA*

Received 20 May 1985

We construct a simple approximation for the Faddeev-Popov determinant in non-abelian gauge models by using sum rules for the density of ghost states. Values are presented for the spectral density and for the determinant, as calculated for the SU(2) gauge model formulated on the hypersphere $S^3$.

## 1. Introduction

We investigate the mechanism by which confinement arises in QCD, by numerical study of the structure of the Coulomb-gauge Yang-Mills hamiltonian. An important factor in the hamiltonian, and a crucial source of non-perturbative effects, is the Faddeev-Popov determinant. This determinant $F$ describes the effective density of physical states associated with a given transverse gauge-field amplitude, in other words, with a given point in the gluon configuration space. Allowed values for the transverse amplitudes must lie in the region bounded by the Gribov horizon, the locus of the first zero of the determinant [1–3].

In general, evaluation of a determinant is a time-consuming numerical task. It might appear, therefore, that the calculation of $F$ could provide a serious technical obstacle to hamiltonian methods. The problem of calculating $F$ nonperturbatively has recently been addressed by Schutte [4], using a cluster expansion. We describe here a simple, direct numerical approach, which gives a quite good estimate for values of $F$. We first calculate a number of the leading zeros, and then use sum rules to estimate the distribution of the remaining zeros. To illustrate the method, we present values of $\ln(F)$ pertaining to the SU(2) gauge model. Our numerical results suggest the possibility that as the momentum cut-off becomes large, zeros become dense almost everywhere beyond the Gribov horizon.

* Permanent address: Ningxia University, Yinchuan, P. R. China.

In the Coulomb gauge ($\nabla \cdot A = 0$) the scalar potential $\Phi$ is determined from the color density $\sigma$ by integration of the Gauss-law constraint equation [5,6]:

$$\left(-\nabla^2 - gA \cdot \nabla\right)\Phi = \sigma. \tag{1.1}$$

The chromoelectrostatic energy is then given by $\frac{1}{2}E^2_{\text{long}} = \frac{1}{2}(\nabla\Phi)^2$.

Our method for non-perturbative numerical calculation uses an expansion in harmonic functions defined over a finite spatial domain. We take the domain to be the hyperspherical surface $S^3$, which provides invariance and topological properties which are superior to those of the more conventional cubical box [3,7]. The expansions are cut off at a momentum index $\Lambda$. We expand the transverse potential in vector harmonic functions as $A(x) = \sum_\alpha A_\alpha V_\alpha(x)$ (the color index is implicit), and expand $\Phi$ and $\sigma$ in scalar harmonics. Removing some laplacian factors and using matrix notation, eq. (1.1) becomes $(1 - D)\ \Phi = \sigma$, where

$$D^{\alpha\beta} = g\sum_\gamma X^{\alpha\beta}_\gamma A_\gamma. \tag{1.2}$$

Here, scalar modes are labeled by greek superscripts and vector modes by greek subscripts. The constants $X$ are products of the structure constants, 3-$j$ symbols, and reduced matrix elements [7].

The Faddeev-Popov determinant is $F = \det(1 - D)$. It is a function only of the variables $A_\alpha$, and is independent of the conjugate variables, the transverse electric field amplitudes. It is therefore possible to explore the properties of $F$ without first solving the Schrödinger equation.

Our method provides an estimate for values of $F(A)$ simultaneously at all points along some line in the space of amplitudes. The direction of this line is defined by choosing some point $A_\alpha$ on the line. For a fixed $A_\alpha$ we calculate eigenvalues $d_i$ of the matrix $D(A)$; the distances to zeros of $F$ along the given line are then determined by scaling $A_\alpha$ to give $d_i = 1$. The largest of the $d_i$ is proportional to the inverse of the distance to the Gribov horizon in the direction $A_\alpha$, while the smallest (most negative) gives the inverse distance in the direction $-A_\alpha$. We use the Lanczos iteration method [8,9] to transform $D$ to a tri-diagonal form. This gives rapid convergence simultaneously to the largest and smallest eigenvalues, so that opposite sides of the allowed Gribov domain can be effectively explored at the same time; we typically obtain convergence for about 10 each of the leading positive and negative eigenvalues before needing to be concerned with round-off errors. The distribution of the remaining eigenvalues is then estimated with the aid of values for $\text{Tr}\, D^\mu$ ($\mu \leqslant 3$). To evaluate these traces, we use formulas which involve the symmetry properties of $S^3$. Finally, we express $\ln(F)$ as an integral over the estimated spectral function; this gives $F$ for all amplitudes proportional to $\pm A_\alpha$.

## 2. Trace calculations

In order to write down the matrix elements and calculate traces, we need to define a more explicit notation. The greek indices $\alpha$, $\beta$, and $\gamma$ used above are composite indices which include the following elements:

$$\alpha = \{(m,n), i, s\} \qquad \text{for a scalar representation } \left(\tfrac{1}{2}s, \tfrac{1}{2}s\right),$$

$$\gamma = \{(p,q), k, v, h\} \qquad \text{for a vector representation } \left(\tfrac{1}{2}(v+h), \tfrac{1}{2}(v-h)\right).$$

The index pairs $(m,n)$, etc. denote the components of the SU(2) × SU(2) representations, and $i, j, k$ are color indices for SU($n$). The quantity $X_\gamma^{\alpha\beta}$ introduced in eq. (1.2) then takes the following form:

$$X_{kvhpq}^{mnis,m'n'js'} = (-1)^{\sigma+m+n+1} f_{ijk} R(s,v,s') \times \begin{pmatrix} \frac{1}{2}s & \frac{1}{2}(v+h) & \frac{1}{2}s' \\ -m & p & m' \end{pmatrix} \begin{pmatrix} \frac{1}{2}s & \frac{1}{2}(v-h) & \frac{1}{2}s' \\ -n & q & n' \end{pmatrix}, \tag{2.1}$$

where*

$$R(s,v,s') = -\frac{1}{\pi}\left[\frac{(s+1)(s'+1)(\sigma-s)(\sigma-s')(\sigma-v)(\sigma+1)}{s(s+2)s'(s'+2)(v+1)}\right]^{1/2} \tag{2.2}$$

is a reduced matrix element [7] divided by laplacian factors from the scalar modes [3], and $\sigma = \frac{1}{2}(s+s'+v+1)$. The $f_{ijk}$ are the SU($n$) structure constants, and the bracket symbols $\begin{pmatrix} \cdots \\ \cdots \end{pmatrix}$ in eq. (2.1) are the conventional 3-$j$ symbols. The sign factor $(-1)^{m+n}$ and the minus signs in the 3-$j$ symbols come from the complex conjugation of the scalar harmonic functions.**

It is now straightforward to calculate the traces. The largest value of $s$ or $v$ included in a specific numerical calculation (the momentum cut-off) is denoted by $\Lambda$. It is easy to check that

$$\mathrm{Tr}\, D^0 = N = (n^2-1)\sum_s (s+1)^2 = \tfrac{1}{6}(n^2-1)\Lambda(2\Lambda^2+9\Lambda+13),$$

$$\mathrm{Tr}\, D^1 = 0. \tag{2.3}$$

For the remaining traces, we sum over each type of index separately. The color sums

* In the course of checking the calculations reported here, we found that the formula given in eq. (29) of ref. [7] is not correct; the factor 2 in the denominator should be omitted.

** In our numerical work, we find it useful to transform to a basis which is explicitly real. This could be done in many ways, and the details are not important.

involve a Casimir operator and provide a factor $n$; with the help also of the 3-$j$ orthogonality relations, we obtain

$$\begin{aligned}\operatorname{Tr} D^2 &= \sum D^{mnm'n'}_{is,js'} D^{m'n'mn}_{js',is} \\ &= ng^2 \sum T_2(v) A^{kpq*}_{vh} A^{kpq}_{vh}, \end{aligned} \tag{2.4}$$

where

$$T_2(v) = \sum_{s,s'} R(s,v,s')^2 [v(v+2)]^{-1}. \tag{2.5}$$

We calculate $\operatorname{Tr} D^3$ in the same way, summing over all the repeated indices, and using the definition of 6-$j$ symbols.

$$\begin{aligned}\operatorname{Tr} D^3 &= \sum D^{mnm'n'}_{is,js'} D^{m'n'm''n''}_{js',ks''} D^{m''n''mn}_{ks'',is} \\ &= \tfrac{1}{2} ng^3 \sum (-1)^{(v+v'+v''+1)/2} f_{ijk} A^{ipq}_{vh} A^{jp'q'}_{v'h'} A^{kp''q''}_{v''h''} T_3(v,h,v',h',v'',h'') \\ &\quad \times \begin{pmatrix} \frac{1}{2}(v'+h') & \frac{1}{2}(v+h) & \frac{1}{2}(v''+h'') \\ p' & p & p'' \end{pmatrix} \\ &\quad \times \begin{pmatrix} \frac{1}{2}(v'-h') & \frac{1}{2}(v-h) & \frac{1}{2}(v''-h'') \\ q' & q & q'' \end{pmatrix}, \end{aligned} \tag{2.6}$$

where

$$\begin{aligned} T_3(v,h,v',h',v'',h'') &= \sum_{s,s',s''} R(s,v,s') R(s',v',s'') R(s'',v'',s) \\ &\quad \times \begin{Bmatrix} \frac{1}{2}(v'+h') & \frac{1}{2}(v+h) & \frac{1}{2}(v''+h'') \\ \frac{1}{2}s & \frac{1}{2}s'' & \frac{1}{2}s' \end{Bmatrix} \\ &\quad \times \begin{Bmatrix} \frac{1}{2}(v'-h') & \frac{1}{2}(v-h) & \frac{1}{2}(v''-h'') \\ \frac{1}{2}s & \frac{1}{2}s'' & \frac{1}{2}s' \end{Bmatrix} \end{aligned} \tag{2.7}$$

and $\begin{Bmatrix} \cdots \\ \cdots \end{Bmatrix}$ denotes a 6-$j$ symbol. The 3-$j$ symbols vanish unless $v+v'+v''$ is odd, which guarantees that $\operatorname{Tr} D^3$ is real.

## 3. Parametrization of $F$

We calculated eigenvalues of the matrix $D$ for points $A_\alpha$ which define lines in the space of amplitudes. A sample of 128 random points was used for each value of $\Lambda$,

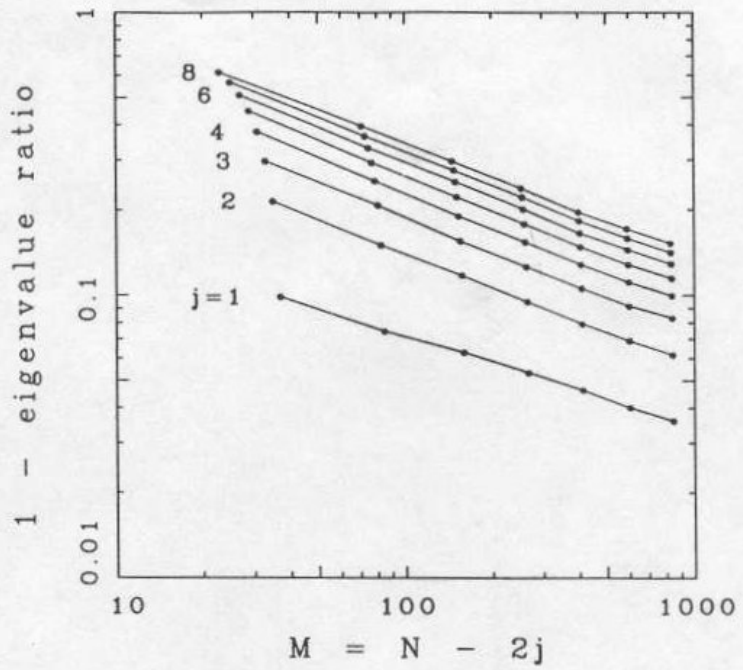


Fig. 1. Relative separation of zeros of $F$.

but as in our previous calculations, the magnitudes of the $A_\alpha$ within the various momentum subspaces were constrained*. The ratios of their squares were fixed by the following formula, which approximates smoothly the results of earlier self-consistent calculations with SU(2)[3]:

$$Q_v^2 = \sum_{\alpha(v)} A_\alpha^2 = N_v \big/ (2W_v) ,$$

$$W_v^2 = (v+1)^2 + (\Lambda^{1/2}+1)^4 \big/ (v+1)^2 ,$$

$$N_v = (\text{number of modes with momentum } v) = 6v(v+2) . \qquad (10)$$

We generally obtained 8 to 15 eigenvalues of each sign, which we denote as $d_{j+}$ or $d_{j-}$, ordered by decreasing magnitude; the two $d_1$ determine where the two rays intersect the horizon.

Fig. 1 shows the values of the quantities $\delta_j = 1 - d_{j+1}/d_1$, averaged over the sample of 256 rays for each value of $\Lambda$, with $2 \leqslant \Lambda \leqslant 8$. The total number of eigenvalues is $N$, as given by eq. (5); $M$ is the number between $d_{j-}$ and $d_{j+}$, and is

* Within each momentum subspace of dimension $N_v$, we chose an ensemble of vectors $A$ with a uniform angular distribution. To generate this ensemble, we applied to an initial vector a sequence of random rotations.

used in the plot because it gives nearly straight lines. The eigenvalue ratios are consistent with $\delta_j \sim \Delta_j M^{\beta}$, where $\beta = -0.35 \pm 0.05$, that is, with $\delta_j \sim \Delta_j/\Lambda$ for large $\Lambda$. This behavior suggests that for infinite $\Lambda$, zeros of $F$ might become dense almost everywhere beyond the horizon.

For each $A_\alpha$, let $\rho(d)$ be the density of eigenvalues. As fig. 1 shows, the average density is least near $d_1$, and we find a roughly linear increase as $d \to 0$. This suggested the following set of approximations using different values of $k$ and $m$:

$$\begin{aligned}
\rho_m^k(x) &= \rho^{\text{true}}(x), && x \le d_{k-} \quad \text{or} \quad x \ge d_{k+}, \\
&= (1 - x/d_{1+}) R_m^k(x), && 0 < x < d_{k+}, \\
&= (1 - x/d_{1-}) R_m^k(x), && 0 > x > d_{k-}, \qquad (11)
\end{aligned}$$

where

$$\rho^{\text{true}}(x) = \sum_j \left[ \delta(x - d_{j-}) + \delta(x - d_{j+}) \right], \qquad (3.3)$$

$$R_m^k(x) = \sum_{\nu=0}^{m} C_{m\nu}^k x^\nu. \qquad (3.4)$$

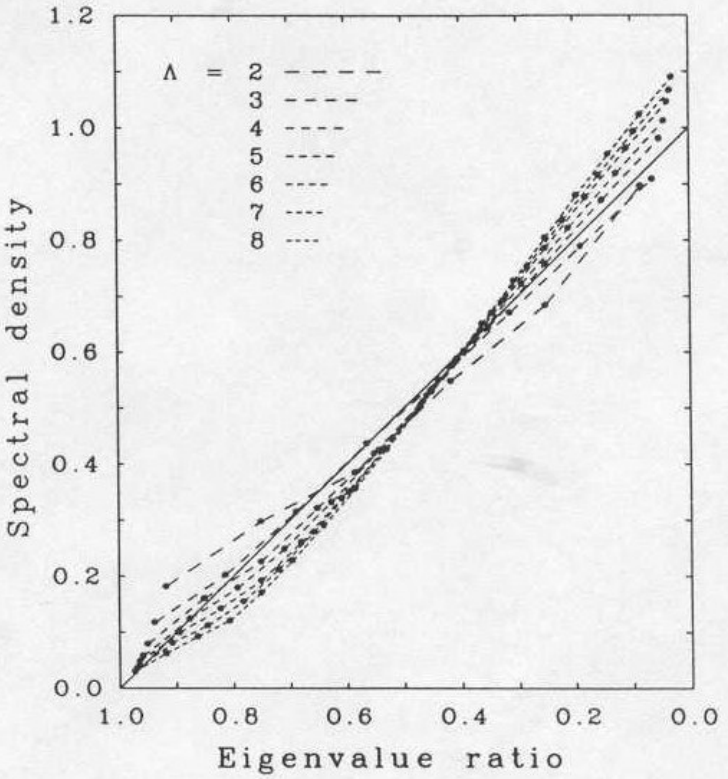


Fig. 2. Relative numbers of eigenvalues versus normalized eigenvalue. The bin widths are shown on the figure.

i.e., we make explicit use of the $k$ largest and smallest eigenvalues, and use an approximate form in between. We also require that $\mathrm{Tr}\, D^{\mu}$, $0 \leqslant \mu \leqslant m$, match the values given in the previous section. Other expressions for the density between $d_{k-}$ and $d_{k+}$ were also tried, but the form given in eq. (3.2) was consistently best. By considering different values of $k$ and $m$, we are able to study the convergence as more information is included.

The sum rules are

$$\mathrm{Tr}\, D^{\mu} = \int \rho_m^k(x) x^{\mu} \mathrm{d}x. \tag{3.5}$$

Via our ansatz these become a set of linear equations for the coefficients $C_{m\nu}^k$ for $0 \leqslant \nu \leqslant m$. The average densities are shown on fig. 2. For each example in our sample of $A_\alpha$ we used all the explicitly known interior eigenvalues, that is, we used the largest possible value of $k$, but the eigenvalues $d_1$ were omitted. We have plotted at the bin centers the integrated densities in bins of widths shown on the figure, using the normalized variable $z = x/d_1$. The densities for positive and negative eigenvalues have been averaged, and divided by $N-2$ to provide a uniform

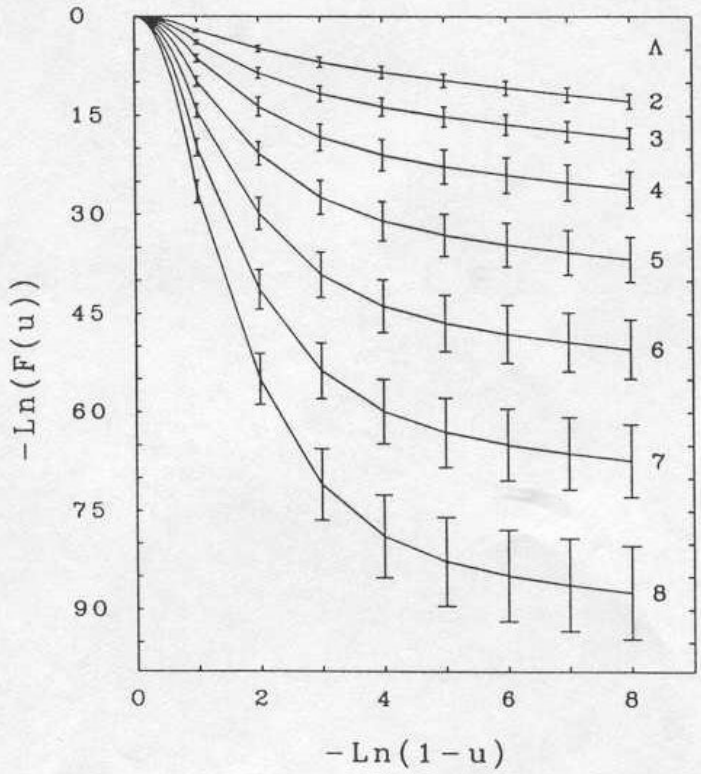


Fig. 3. For the indicated values of $\Lambda$, $\ln(F)$ is plotted against $\ln(1-u)$. The error bars indicate the r.m.s. fluctuations in a sample of 128 directions of the $A_\alpha$ (most of the fluctuation, especially for small $u$, arises simply from variation in the horizon distance.)

normalization. The bin widths were chosen so that the last of the explicitly-calculated eigenvalues was nearly always in the third or fourth bin. Note that the deviation from linearity is not great.

We can now calculate $\ln(F)$. Let $A$ be the (signed) distance from the origin of the gluon coordinate space along the line $A_\alpha$, and let $u = Ad_{\pm}$. At the horizon, $u = 1$. Then:

$$\ln F(A) = \int \ln(1 - Ax)\rho_m^k(x)\,dx. \tag{3.6}$$

Thus, having found the $C_{m\nu}^k$ for given $k$ and $m$, we can calculate $\ln F(A)$ for any $A$ with little effort. Fig. 3 shows the averaged results of such calculations, using $m = 3$ and the maximum available $k$, plotted against $\ln(1 - u)$.

To study the behavior of series of approximations, we varied $k$ from one to about ten (we usually obtain that many before round-off error spoils accuracy) and $m$ from zero to three (higher degree would require $\mathrm{Tr}\,D^4$, etc.). For each value of $\Lambda \leqslant 5$, we checked our method by explicit calculation of $F$ using a sample of 99 directions of the $A_\alpha$. We find increasing accuracy for larger values of $k$ and $m$, and apparent

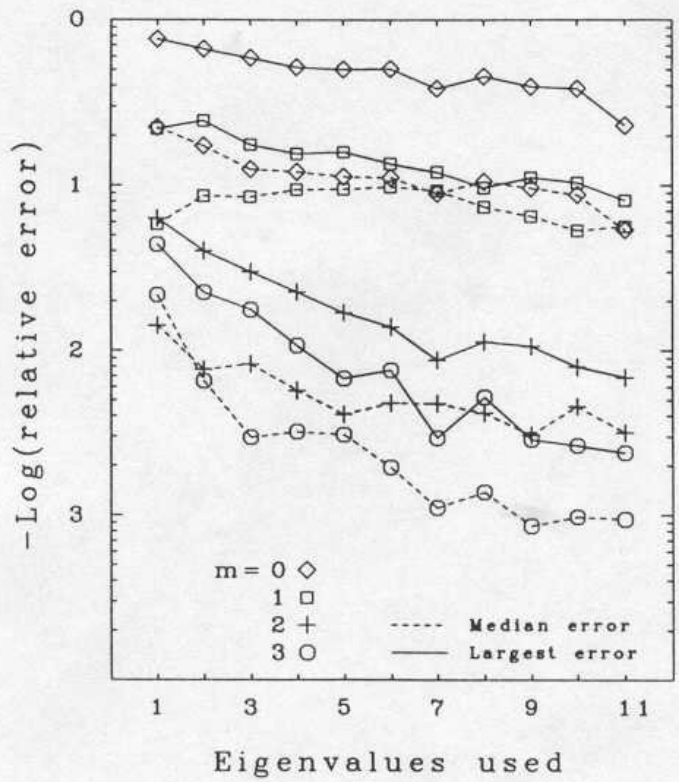


Fig. 4. Logarithm (base 10) of the relative error in $\ln(F)$ versus $k$, the number of eigenvalues used on each side, for $\Lambda = 5$ and $-\ln(1 - u) = 4$ ($u \sim 0.98$). The solid lines show the largest error, and the dashed lines show the median error, for the indicated values of $m$ in a sample of 99 directions of the $A_\alpha$.

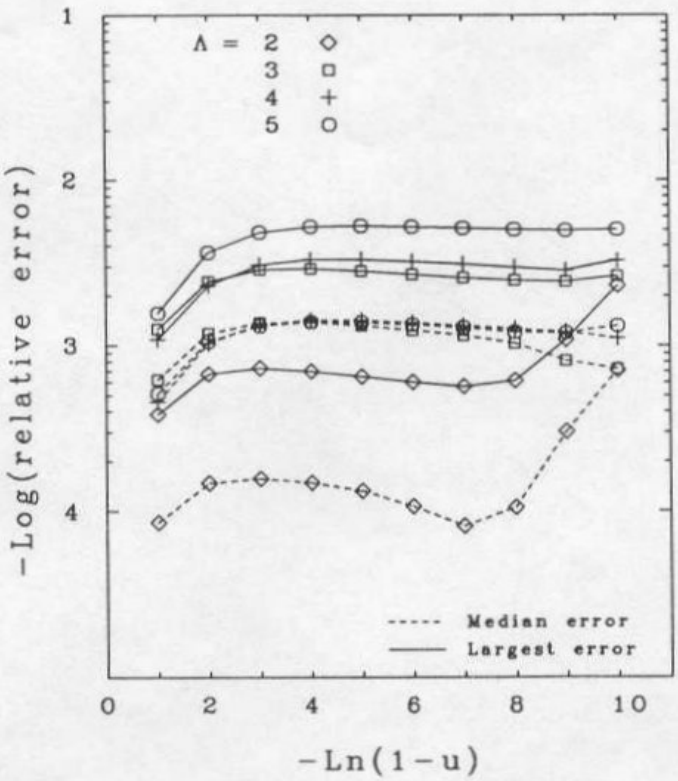


Fig. 5. Logarithm of the relative error in $\ln(F)$ versus $\ln(1-u)$, for $k=8$ and $m=3$. A sample of 99 directions of the $A_\alpha$ was used for each of the indicated values of $\Lambda$.

convergence. Fig. 4 shows the relative error in $\ln(F)$ versus $k$, for $\Lambda=5$ and $u=1-e^{-4}\sim 0.98$, which was chosen as a typical expectation value in the vacuum state. As can be seen in fig. 5, the accuracy is about the same for all relevant values of $u$ (i.e., neither close to the origin nor very close to the horizon). For each example in our sample, at least 8 eigenvalues of each sign were available, and we show in fig. 5 the relative error versus $\ln(1-u)$ for $k=8$.

We thank I. Barbour and H. W. Wyld for helpful advice about the Lanczos method. This work was supported by the US Dept. of Energy under contract DE-AC02-76ER0306.

## References

[1] V.N. Gribov, Nucl. Phys. B139 (1978) 1
[2] D. Zwanziger, Nucl. Phys. B209 (1982) 336; Phys. Lett. 114B (1982) 337
[3] R.E. Cutkosky, Phys. Rev. Lett. 51 (1983) 538 and 1603(E); Phys. Rev. D30 (1984) 447
[4] D. Schutte, Phys. Rev. D 31 (1985) 810;
B. Faber, H. Nguyen and D. Schutte, Bonn preprint (1985)

[5] N.H. Christ and T.D. Lee, Phys. Rev. D 22 (1980) 939
[6] T.D. Lee, Particle physics and introduction to field theory (Harwood Academic, New York, 1981) pp. 443, 532
[7] R.E. Cutkosky, J. Math. Phys. 25 (1984) 939
[8] C.C. Paige, J. Inst. Math. Appl. 10 (1972) 373
[9] J. Cullum and R.A. Willoughby, Sparse matrix proceedings, ed. I. Duff and G. Stewart, (SIAM, Press, 1979) 220